1   **New Insights into the Crystallographic Disorder in the Polymorphic**

2   **Forms of Aspirin from Low-frequency Vibrational Analysis**

3

4   Qi Li[a], Andrew D. Bond[b], Timothy M. Korter[c], and J. Axel Zeitler[a][*]

5

6   [a]Department of Chemical Engineering and Biotechnology, University of Cambridge, Philippa

7   Fawcett Drive, Cambridge, CB3 0AS, UK.

8   [b]Yusuf Hamied Department of Chemistry, University of Cambridge, Lensfield Road, Cambridge,

9   CB2 1EW, UK.

10   [c]Department of Chemistry, Syracuse University, 1-014 Center for Science and Technology,

11   Syracuse, NY 13244, USA.

12

13   [*]Corresponding author

14   **E-mail:** jaz22@cam.ac.uk

15   **Phone:** +123 (0) 123 4445556

16   **Fax:** +123 (0) 123 4445557

**Abstract**

18    Terahertz time-domain spectroscopy (THz-TDS) is applied to two polymorphs of acetylsalicylic

19    acid (aspirin), and the experimental spectra are compared to lattice dynamical calculations using

20    high accuracy density functional theory (DFT). The calculations confirm that forms I and II have

21    very close energetic and thermodynamic properties, and also that they show similar spectral

22    features in the far-infrared region, reflecting the high degree of similarity in their crystal

23    structures. Unique vibrational modes are identified for each polymorph which allow them to be

24    distinguished using THz-TDS measurements. The observation of spectral features attributable to

25    both polymorphic forms in a single sample, however, provides further evidence to support the

26    hypothesis that crystalline aspirin typically comprises intergrown domains of forms I and II.

27    Differences observed in the baseline of the measured THz-TDS spectra indicate a greater degree

28    of structural disorder in samples of form II. Calculated Gibbs free energy curves show a turning

29    point at 75 K, inferring that form II is expected to be more stable than form I above this

30    temperature, as a result of its greater vibrational entropy. The calculations do not account for any

31    differences in configurational entropy that may arise from expected structural defects. Further

32    computational work on these structures, such as ab initio molecular dynamics (AIMD), would be

33    very useful to further explore this perspective.

34

# 1   Introduction

The crystal structure of one of the most well-known analgesics, acetylsalicylic acid, commonly referred to under its trade name aspirin, was first characterised by Wheatley in 1964.[1] After the initial crystal structure was determined, it was widely discussed whether other crystal forms of aspirin may exist, but it was not until 2005 that Vishweshwar et al. reported the crystal structure of aspirin form II.[2] The form II structure had been identified as an energy minimum by Ouvrard and Price[3] in a crystal-structure prediction exercise, but sub-optimal features of the experimental structure determination left doubts over the validity of the crystal structure and the existence of form II as a discrete polymorph.[4] The origin of these difficulties was explained by Bond et al., who showed that aspirin forms I and II exist as intergrown single crystals, comprising domains of both structure types.[5] Reproducible crystallisation of form II remained challenging, but it was shown in 2010 that domains of the second polymorph of aspirin are introduced reliably in the presence of aspirin anhydride during the crystallisation process.[6] More polymorphs of aspirin have since been discovered.[7]

In this paper, we focus on the closely-related aspirin polymorphs, form I and form II. There are considerable similarities in their respective crystal structures, which permit the observed intergrowth behaviour. Figure 1 shows the projections of the two polymorphs along the a, b and c axis. The structures are polytypes [8], having consistent layers lying in the bc planes. For the two forms, the difference is seen in the arrangement of these layers along the a axis. The relationship between the structures can be viewed as a shift of neighbouring layers by half a unit-cell length along the c axis (as can be seen in the a axis projection), or alternatively as a reflection of every second layer perpendicular to the b axis. Given the observed intergrowth behaviour, it is evident that the two arrangements must have closely comparable energies. Computational work using density functional theory (DFT) has indicated that the two forms exhibit only a subtle energetic difference, and it was suggested that the two polymorphs were virtually degenerate.[9] Later on, Reilly and Tkatchenko applied a many-body dispersion approach with DFT to investigate their energetic differences at room temperature, which inferred that the stability of form I was due to the coupling of low-frequency phonon modes and collective electronic fluctuations. [10] A recent work of Vaksler *et al.* proposed a new method to study the mechanical properties using quantum chemical calculations constituted of two steps: analysis of the pairwise interactions between molecules and modelling displacement between strongly

68   bound fragments. [11] The results identified the crystallographic c axis, within the region between

69   the common planes of the polytypes, as the most likely direction for shear deformation to occur.



70
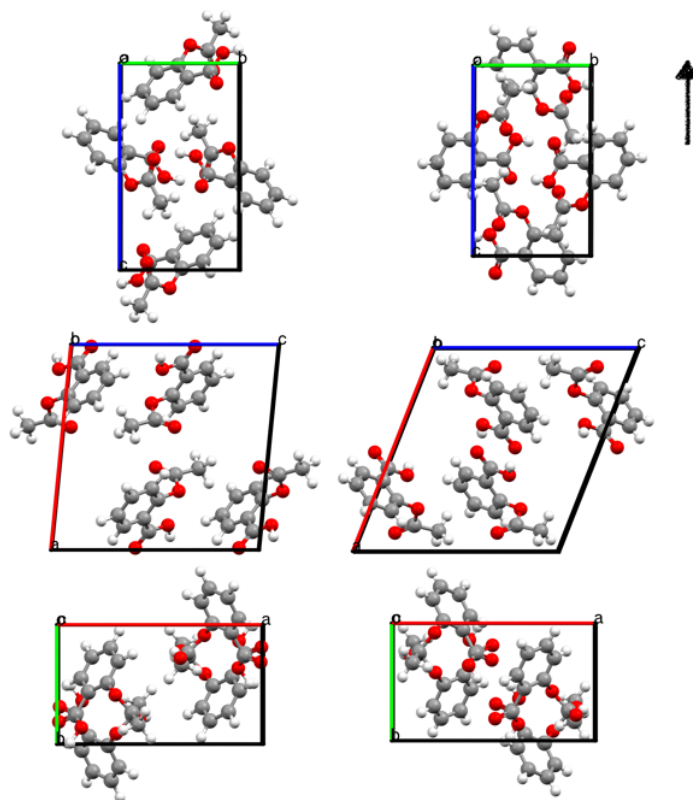
71   **Figure 1:** Projections of aspirin form I (left) and form II (right), viewed from a, b, and c axis (from top to bottom).

72        Even though crystals are defined as well-organised and ordered systems, defects and

73   dislocations are commonly encountered in crystalline materials. The influence of defects, for

74   example on the properties of metals, has been widely studied. It is well known that defects can

75   also affect the performance of molecular materials such as their mechanical stability. [12] The subtle

76   differences in crystal structure between the two aspirin forms and the comparable energetic

77   stabilities challenge the view of distinct polymorphs and make this an interesting model system

78   for investigating the effect of disorder and the structural dynamics in organic molecular crystals

79   beyond their perfect structures. Chan et al. have reported a detailed structural study of aspirin

80   crystals, with disorder models fitted to diffuse X-ray scattering data. [13] These results confirm that

81   crystals of form I are well ordered, but that form II crystals contain stacking faults corresponding

82   to the form I interlayer arrangement, which aggregate to form included regions of the form I

83  structure. Hence, "pure" form II is generally not encountered, and may not be experimentally
84  attainable.

85      By combining vibrational spectroscopy in the far-infrared region, measured by terahertz time-
86  domain spectroscopy (THz-TDS), and ab initio DFT simulations under periodic boundary
87  conditions, we seek here to obtain further insight into the nature of aspirin form I/II
88  polymorphism. The measurement of vibrational dynamics complements the structural
89  characterisation from crystallographic techniques, while the solid-state DFT methods provide a
90  powerful route for interpretation of the terahertz spectra. These methodologies have previously
91  been applied to study a wide range of organic molecular crystals, including polymorphs of
92  pharmaceutical drug molecules.[14–17] THz-TDS probes weak interactions within molecular
93  crystals, but due to the complexity of the motions at terahertz frequencies, not least given the
94  strong coupling between large amplitude external and internal motions, the spectra are difficult to
95  interpret without the complementary DFT method. The terahertz spectrum of aspirin form I has
96  previously been measured by Laman, Harsha and Grischkowsky using a bespoke THz-TDS
97  setup, where thin films of crystals were grown directly onto the surface of an aluminium parallel
98  plate waveguide structure.[18] This method has the advantage that no scattering occurs when the
99  terahertz electric field propagates along the surface of the waveguide and the effervescent field
100 can interact very efficiently with the crystalline film. As a result, the line width of the vibrational
101 modes is dramatically sharpened compared to conventional transmission spectroscopy of a
102 polycrystalline sample (Figure S1). However, the requirement to crystallise the sample directly
103 onto the flat aluminium plate waveguides in the form of a thin film restricts the application of the
104 method for detailed investigation of complex polymorphism where such constraints in
105 crystallisation conditions limits the accessible solid-state forms. Therefore, we apply
106 transmission measurements on pellets containing polycrystalline particles of the two
107 polymorphic forms of aspirin using a commercial terahertz spectrometer.

108

## 2    Experimental section

### 2.1    Materials

Commercial aspirin form I of USP grade was acquired from Sigma-Aldrich (Gillingham, UK) and used as received. Form II was prepared following the procedure described by Bond et al. through crystallisation from the organic solution of form I in the presence of aspirin anhydride.[6] A bulk solid mixture of 9 g aspirin and 1 g aspirin anhydride was prepared, and divided into 10 x 1 g portions in separate vials. The solid in each vial was dissolved in 3 ml tetrahydrofuran (THF) with shaking, then left to evaporate under ambient conditions. X-ray powder diffraction (XRPD) was used to confirm the crystalline structure of all samples prior to any subsequent terahertz spectroscopy experiments.

### 2.2    X-ray powder diffraction (XRPD)

X-ray powder diffraction measurements were carried out on a Panalytical XPert Pro diffractometer in Bragg-Brentano geometry, using non-monochromated CuK$\alpha$ radiation ($\lambda_{ave}$ = 1.5418 Å). Samples were prepared on glass flat-plate sample holders and data were measured over the range $2\theta$ = 3-40°. Due to the polytypic relationship between the crystal structures, the diffraction patterns of aspirin form I and II are closely comparable (50% of the reflections are identical). Form II domains are indicated by signature peaks at $2\theta \approx$ 16.0, 19.2 and 26.0°.[5]

### 2.3    Terahertz time-domain spectroscopy (THz-TDS)

The THz-TDS measurements were performed in transmission using a commercial spectrometer (TeraPulse 4000, TeraView Ltd., Cambridge, UK) equipped with a cryostat (Janis, Massachusetts, USA) and an attached temperature controller (Lakeshore 330, Ohio, USA). The set up was used to acquire measurements in the temperature range between 80 and 400 K.

Due to the strong absorption from pure crystals, polycrystalline aspirin powder was diluted in polyethylene (PE) powder (Induchem, Volketwil, Switzerland) to a 5 % w/w concentration using an agate mortar and a pestle by gentle mixing. The powder mixture was then compressed into a pellet of 13 mm diameter using a hydraulic press (Specac Ltd., Kent, UK) at a load of 2 tons, and a blank PE pellet was prepared in the same way to be used as a reference. For each sample, 1000

137    waveforms were acquired and averaged with a spectral resolution of 0.94 cm$^{-1}$. A spectrum was

138    first acquired at room temperature to check if the sample pellet was at the proper concentration.

139    The whole system was then cooled to 80K with liquid nitrogen to acquire a spectrum at low

140    temperature that would be more comparable with the simulated spectrum from the DFT

141    calculations.


142    **2.4    Density functional theory calculations**


143    The DFT simulations were performed using the CRYSTAL17 software package.[19] The published

144    crystallographic data from the Cambridge Structural Database (CSD) (ACSALA07; ACSALA17)

145    were used to set the initial atomic positions and lattice parameters.[13,20,21] The subtle differences

146    between the two polymorphs required very strict parameters for the best differentiation. The

147    "extra extra large" grid (XXLGRID) was used to generate 100 k-points in reciprocal space

148    (SHRINK=7) and the tolerance of bielectronic coulomb and Hartree-Fock (HF) exchange

149    integrals were set to $10^{-12}$, $10^{-12}$, $10^{-12}$, $10^{-12}$ and $10^{-24}$ (TOLINTEG). The atomic centered triple-$\xi$

150    Ahlrichs' VTZ basis set (with polarisation)[22] and the PBE density functional[23] with Grimme-D3

151    London dispersion correction[24,25] were applied with a three body Axilrod-Teller-Muto repulsion

152    term (ABC)[26]. The energy convergence criterion for the geometry optimisation was set at $10^{-8}$

153    Hartree, and $10^{-10}$ Hartree for the frequency analysis. The default DIIS convergence accelerator

154    was applied. In addition, two displacements for each atom along each Cartesian direction were

155    calculated for the phonon modes (NUMDERIV=2) and the IR intensities were calculated based

156    on the Berry phase method.[27,28] The cohesive energies of both forms were calculated by

157    subtracting the isolated molecular energy from the total solid-state energy considering the basis

158    set superposition error (BSSE), which originates from the finite basis sets.[29] Select normal modes

159    were selected and the corresponding geometries were scanned along the eigenvectors to obtain

160    more information on these modes (SCANMODE). The Gibbs free energy as well as other

161    thermodynamic properties were calculated from 7 K to 300 K for each structure.


162

## 163  3    Results and discussion

### 164    3.1    X-ray powder diffraction (XRPD)

165    The bulk solids from the crystallisation trials contained differing degrees of form II domains, as

166    indicated by the relative intensities of the signature form II peaks in the XRPD patterns (Figure

167    S2). Trace aspirin anhydride was also detected in most samples. The variability in the

168    crystallization outcome is attributed principally to (deliberate) inhomogenous mixing of the

169    initial aspirin/aspirin anhydride solid sample. Three samples were selected for further analysis,

170    which contained minimum quantities of aspirin anhydride and a range of form II peak intensities.

171    The sample referred to as "form I" shows no evidence of form II peaks in the XRPD, "low purity

172    form II" shows form II peaks of intermediate intensity, and "high purity form II" shows the most

173    intense form II peaks (Figure 2). Here, "purity" refers to the polymorphic composition. Hence,

174    the form I sample straightforwardly represents the aspirin form I structure, the high purity form

175    II sample is the best available representative of the form II structure, and the low purity form II

176    sample comprises the form II structure with a more substantial fraction of form I domains.
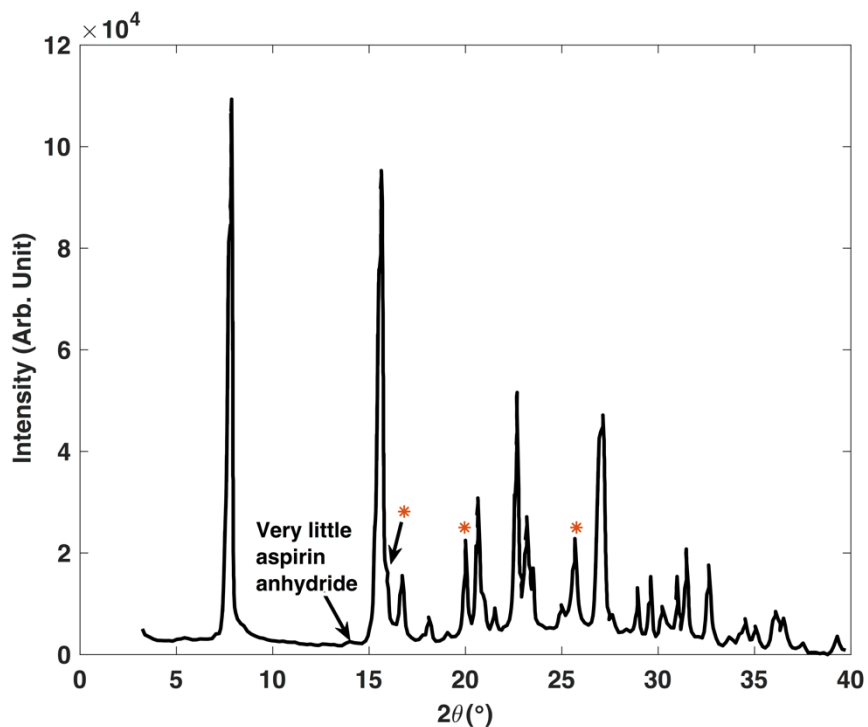


177

178    **Figure 2:** XRD pattern of the high purity form II.

## 3.2   Terahertz time-domain spectroscopy (THz-TDS)

The maximum absorption coefficient ($\alpha_{max}$) was determined by the dynamic range of the terahertz signal.[30] It was checked qualitatively for the experimental results to make sure that the absorption was within the accessible range. Figure S3 shows that the absorption did not exceed the dynamic range of the instrument for frequencies up to 3 THz. Therefore, the spectra obtained for the two polymorphs were valid for further analysis.

Figure 3 shows the experimental spectra of form I and the two form II samples at 80 K. The overall resemblance of all parts of the spectra reflects the close structural similarity between the two forms, which is not generally common in other polymorphic systems. In order to facilitate comparison, the spectra were normalised relative to the peak at 1.8 THz, which is a pronounced feature in both forms (Figure 3). The reason for choosing this feature will be explained in the following section of computational results. In general, the peaks of form II appeared relatively broader than those of form I, which may reflect the inherent disorder expected for form II. The three main differences are pointed out in Figure 3: (i) the feature at around 1.5 THz is considerably more intense in the form II samples than in form I; (ii) around 2.0 THz, the spectra of the form II samples clearly show peak broadening and merging; (iii) the form II samples show a shoulder on the high frequency flank of the peak just before 2.5 THz.
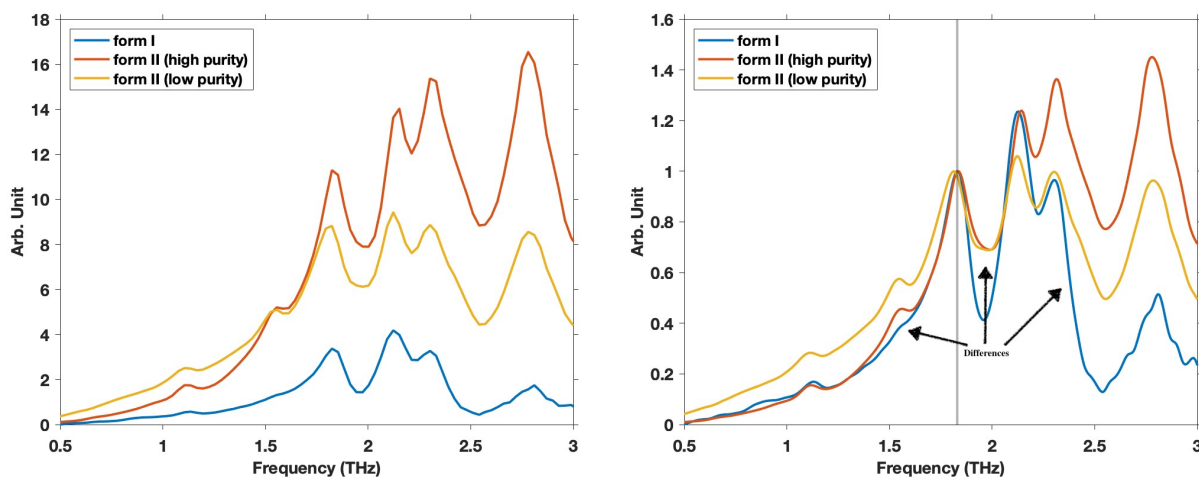


**Figure 3:** The experimental spectra (left) of aspirin form I (blue), form II with high polymorphic purity (red), and form II with low polymorphic purity (yellow). The spectra (right) are normalised relative to the feature at 1.8 THz.

### 3.3 Optimisation of the crystal structures

200 The experimental crystal structures of both polymorphic forms were optimised using the settings

201 described in the Experimental section and compared with their published experimental data at

202 100 K and 300 K respectively (as shown in Table S1 and S2). The relative errors between

203 experimental and optimised structure are small, demonstrating the accuracy of the calculations.

204 As expected, the calculated physical properties of the two polymorphs (Table 1) show only

205 marginal differences. The total lattice energy of form II is calculated to be 0.293 kJ mol$^{-1}$ higher

206 than form I, which implies that form I is marginally the more energetically stable state. The

207 energy difference increases to 1.609 kJ mol$^{-1}$ when considering also the zero-point energies. The

208 cohesive energy ($E_{cohesive}$ per molecule) of form I is predicted to be 0.560 kJ mol$^{-1}$ lower than

209 form II prior to any correction for BSSE, but rises to 0.035 kJ mol$^{-1}$ higher than form II after

210 BSSE correction. A noticeable difference is that the entropy of form I is predicted to be smaller

211 than that of form II. It should be noted that this refers to vibrational entropy, calculated for the

212 idealised form I and form II crystal structures. The calculations do not quantify configurational

213 entropy associated with the structural disorder described for form II single crystals.

214

215 **Table 1:** Comparison of the properties of the two polymorphs (form I-form II). The entropy and heat capacity listed

216 in the table are values predicted at 298.15 K and atmospheric pressure.

|  | Form I | Form II | Difference |
|---|---|---|---|
| **Energy (×10$^6$ kJ mol$^{-1}$)** | -6.80803637 | -6.80803608 | -0.293 |
| **Volume (Å$^3$)** | 834.803 | 832.476 | 2.328 |
| **Density (g cm$^{-3}$)** | 1.433 | 1.437 | -0.004 |
| **E$_{cohesive}$ (kJ mol$^{-1}$)** | 205.092 | 205.652 | -0.560 |
| **E$_{cohesive}$ with BSSE (kJ mol$^{-1}$)** | 10.285 | 10.250 | 0.035 |
| **Zero-point energy (kJ mol$^{-1}$)** | 1617.261 | 1615.945 | 1.316 |
| **Entropy (J mol$^{-1}$ K$^{-1}$)** | 862.097 | 875.594 | -13.497 |
| **Heat capacity (J mol$^{-1}$ K$^{-1}$)** | 785.492 | 785.638 | -0.146 |

217

### 3.4 Frequency analysis

The simulated vibrational spectra were calculated for the optimised crystal structures, and are compared with the experimental results in Figure 4 (the experimental results of the high purity form II are used onwards for further analysis). Figure 5 shows the simulated spectra of both forms with the bandwidth set to 1 cm$^{-1}$ in order to display each feature for a clearer comparison. As shown, the peak at around 1.8 THz is predicted for both forms with comparable intensities, hence the decision to normalise the experimental spectra relative to that feature in Figure 3. The three circled areas correspond to the differences identified between the experimental spectra: (i) the feature at 1.53THz is predicted only for form II, which explains why the peak is more pronounced in the spectra of the form II samples; (ii) the merging of the peaks just below 2.0 THz in form II can be explained by the extra feature predicted on the high frequency side of the intense peak at 1.82 THz; (iii) the broad shoulder at 2.5 THz in the experimental spectra of the form II samples matches well with the two less intense peaks at 2.37 and 2.58 THz predicted for form II. Overall, the simulated spectra show a greater degree of difference between the two polymorphs compared to that observed in the experimental spectra. One way to explain this could be the expectation that the form II samples are intergrown with form I domains. To explore this possibility further, a small amount of the "high purity" form II sample was used to spike the bulk form I sample and vice versa. This resulted in even closer similarity between the experimental spectra. As a final observation, the anticipated structural disorder in the form II samples would be expected to result in non-coherent and less pronounced vibrational motions, which are suggested by the increasing of the baseline in the THz spectra.[31]
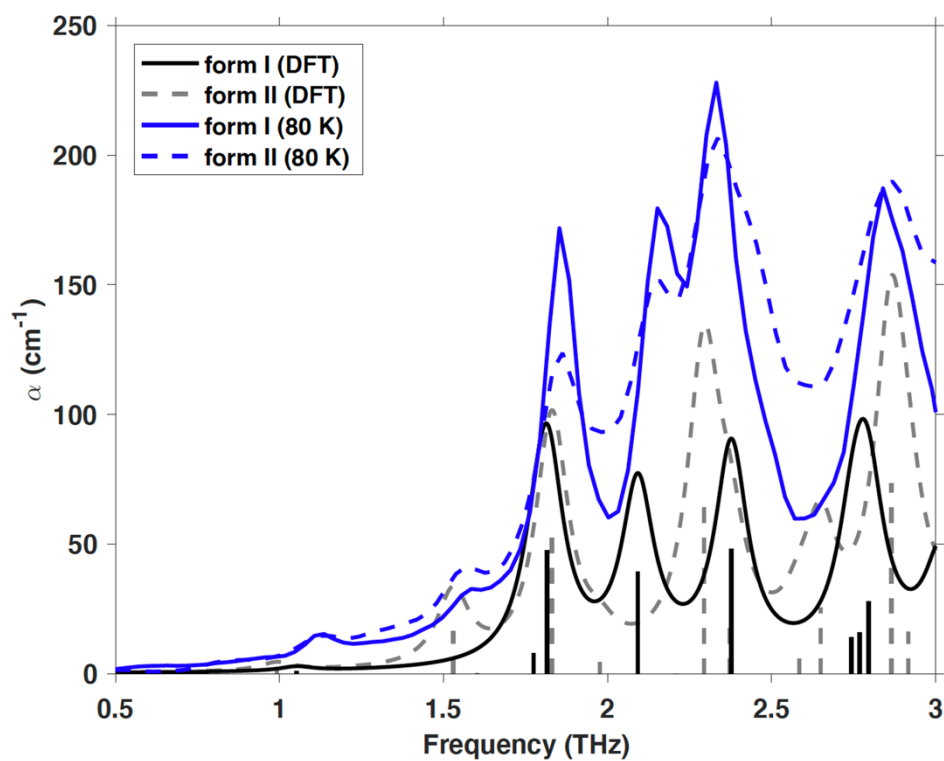
**Figure 4:** The simulated spectra of aspirin form I (black solid) and form II (grey dashed); The experimental spectra of aspirin from I (blue solid) and form II (blue dashed).
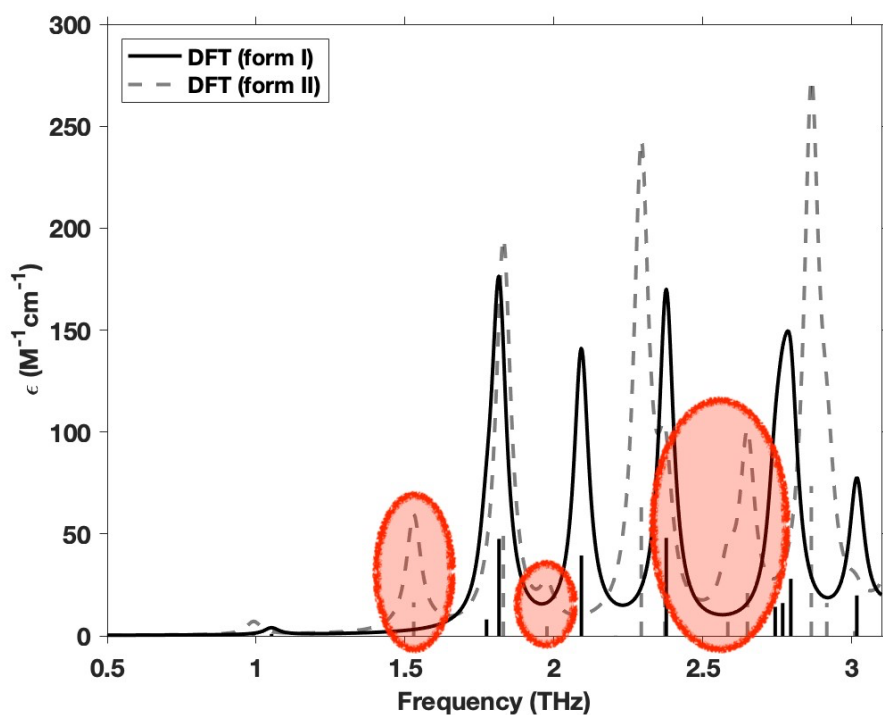
243         **Figure 5:** The simulated spectra of form I and II when bandwidth was set to 1 cm⁻¹.

244         To quantify the comparison, the experimental spectra were fitted in Matlab with the spectral

245 features constrained to the frequencies predicted by the simulations, where the peaks were fitted

246 to Lorentzian functions and the baseline was fitted to a power law (Eqn 1).

$$y = \sum_n \frac{A_n}{\left(1 + \left(\frac{x - f_{c_n-d}}{g_n}\right)^2\right)} + Bx^a + c \tag{1.}$$

247

248 where $A_n$ is the amplitude of the peak, $g_n$ is the peak width, $f_{c_n}$ is the predicted frequency of the

249 peak, d is the relative shift between the simulated active modes, and $Bx^a + c$ was used to fit the

250 baseline. Application of the shift d is common practice and is mainly due to the difference in

251 temperature between the experimental (80 K) and simulated (0 K) results as well as additional

252 effects of anharmonicity. The fits are shown in Figure 6, and the resulting parameters are shown

253 in Table 2. The highlighted features in both samples are not predicted in the corresponding form,

254 but rather in the other polymorph. The fact that it is possible to fit the experimental spectra very

255 closely using this methodology, but that both spectra contain residual features indicative of the

256 other polymorphic form, substantiates the hypothesis that the two polymorphs are intergrown in

257 the samples analysed, and furthermore demonstrates that this feature can be detected by the THz

258 measurements. It is also notable that the baseline fitting parameters of form II in Table 2 are

259 larger than those required for form I, consistent with the expectation that the form II sample is

260 more disordered. This can also be reflected from the wider peak width in form II on average, as

261 peak broadening is a significant effect to the terahertz absorption spectra caused by disorder in

262 crystalline materials.[32,33]
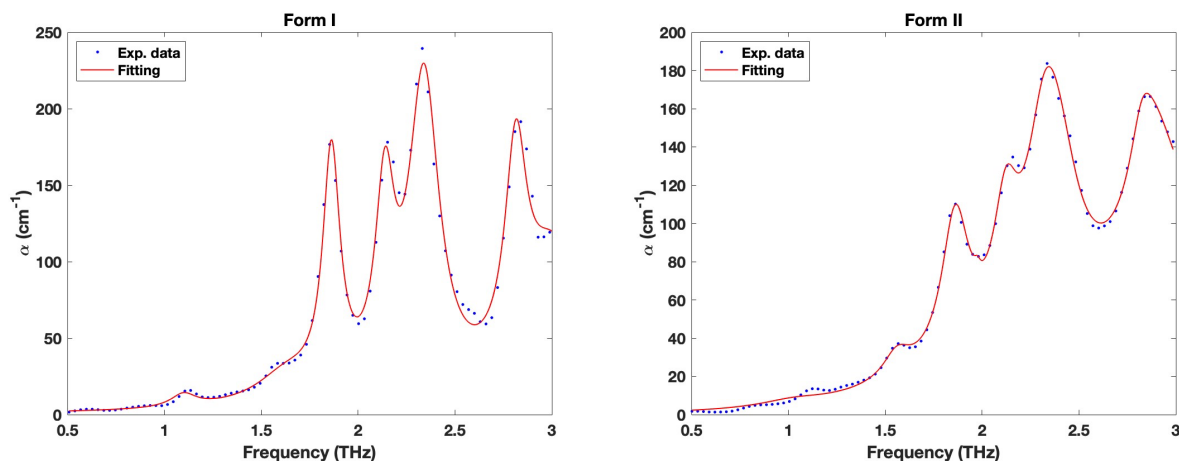
**Figure 6:** Aspirin form I (left) and form II (right) experimental spectra fitted with the Lorentzian functions and the power law with fixed simulated modes.

**Table 2:** The power law fitting parameters for aspirin form I and form II (top). The Lorentzian fitting parameters of form I (bottom left) and form II (bottom right). Features highlighted with an asterisk are not predicted in the corresponding form but rather in the other polymorph.

|  | B | a | c | d (THz) | d (cm$^{-1}$) | R$^2$ |
|---|---|---|---|---|---|---|
| **Form I** | 0.0164 | 0.364 | 0.00285 | 0.0476 | 1.59 | 0.991 |
| **Form II** | 1.04 | 4.14 | 0.150 | 0.0329 | 1.10 | 0.999 |

| fc$_n$ (THz) | A$_n$ (cm$^{-1}$) | g$_n$ |
|---|---|---|
| 1.05 | 8.82 | 0.0772 |
| 1.53* | 18.2 | 0.164 |
| 1.81 | 157 | 0.0564 |
| 2.10 | 123 | 0.0600 |
| 2.29 | 206 | 0.0959 |
| 2.38 | 0.285 | 0.274 |
| 2.77 | 134 | 0.0675 |
| 3.02 | 99.5 | 0.198 |

| fc$_n$ (THz) | A$_n$ (cm$^{-1}$) | g$_n$ |
|---|---|---|
| 1.00 | 3.67 | 0.209 |
| 1.53 | 14.5 | 0.115 |
| 1.83 | 75.9 | 0.0876 |
| 1.98 | 3.58 | 0.0823 |
| 2.09* | 60.3 | 0.118 |
| 2.29 | 91.5 | 0.0848 |
| 2.37 | 50.0 | 0.128 |
| 2.79* | 45.4 | 0.538 |
| 2.86 | 40.3 | 0.134 |

274   It is evident in Figure 6 that the first peak of form II at 1.0 THz is not fitted as well as the

275   other features. Therefore, further calculations were performed to examine the energies of the

276   structures with the atoms displaced in steps along the eigenvectors corresponding to the first

277   spectral features of each form. Figure 7 shows that the difference between the energy calculated

278   with the harmonic approximation and the real total energy of form II was much larger than that

279   of form I. This implies that the influence of anharmonicity is much larger for the first peak of

280   form II than for form I, which can account for the less effective fitting that is observed. In

281   addition, it was found that the methyl groups (-CH$_3$) in form II were much more active than in

282   form I within the whole low-frequency range (0.5 THz - 3 THz), showing both rotation around

283   the C–CH$_3$ bond and greater motion of the entire acetyl group. This can be related to differences

284   in the local environments of the CH$_3$ groups, which include C–H⋯O and C–H⋯π intermolecular

285   contacts (Figure 8). Two out of three such contacts (within the layers common to the polytypes)

286   are directly comparable in the two polymorphs, but the "interlayer" C–H⋯O contact in form I is

287   shorter and closer to linear than that in form II. Hence, the CH$_3$ groups in form I adopt an

288   approximately symmetrical position between two neighbouring O atoms in form I, compared to

289   an asymmetrical arrangement in form II. The results confirm the observations reported in the

290   early work of Reilly and Tkatchenko.[10]

291



15
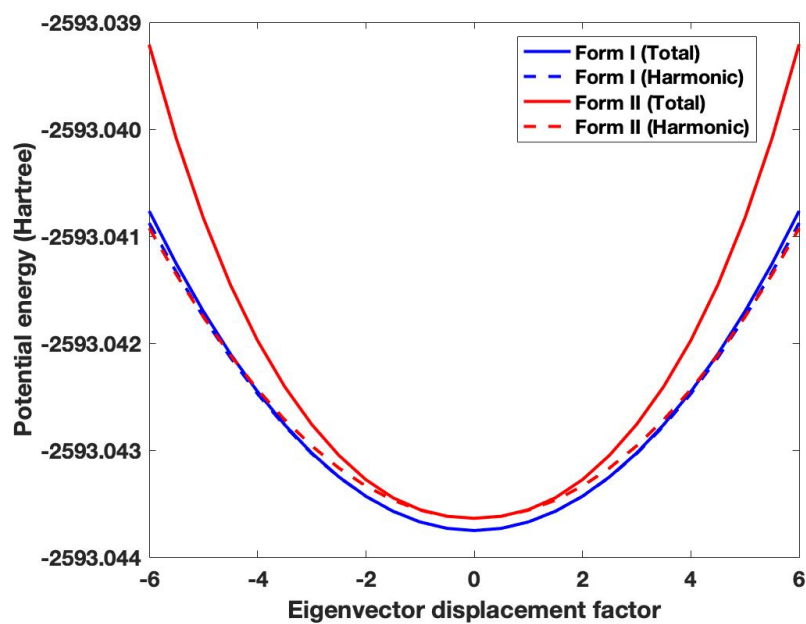
292　**Figure 7:** The energy curves of form I (blue) and form II (red) around the equilibrium position. The solid lines
293　represented the total energies of the geometry at each position, and the dashed ones were for the energies calculated
294　based on harmonic approximation.
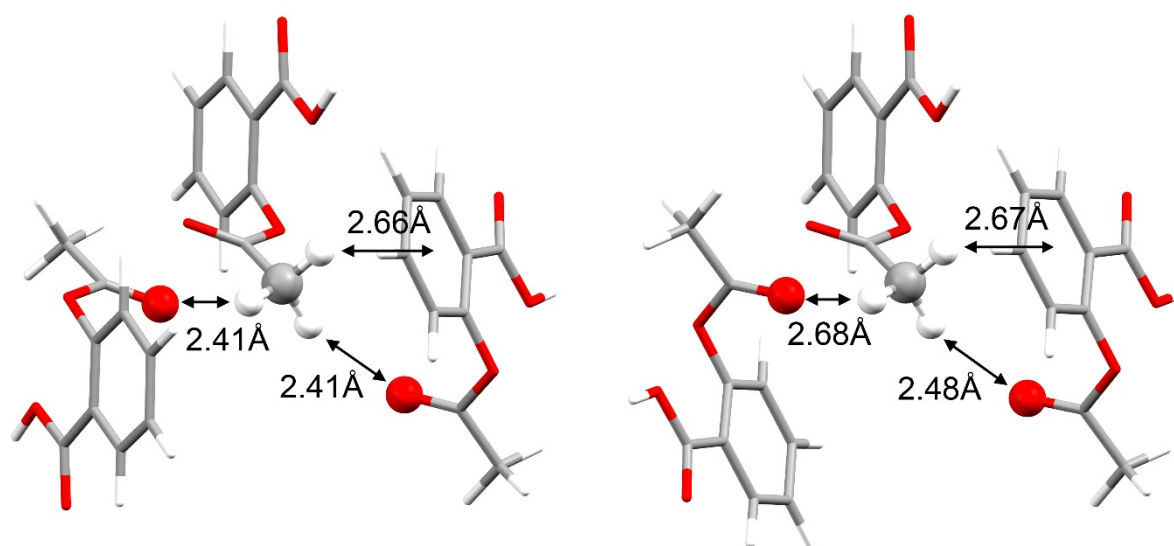


295　**Figure 8:** C–H⋯O and C–H⋯π intermolecular contacts within the optimised crystal structures of form I (left) and
296　form II (right). The central and right-hand molecule in each diagram lie within the consistent 2-D layers of the
297　polytypes, while the different C–H⋯O contact is formed between layers.

## 3.5　Free energies of the polymorphs

299　　　In Section 3.3 (Table 1), it was shown that the total lattice energy of form I is calculated to be

300　marginally lower than that of form II at absolute zero. To further investigate the relative stability

301　of the polymorphs at real temperatures, the Gibbs free energy curves of both forms were

302　calculated from 7K to 300K (shown in Figure S4 and the lower bound being limited by the

303　CRYSTAL17 software package[28]). A turning point is predicted at 75K, where the Gibbs free

304　energy of form I becomes larger than that of form II, which infers that form II is more stable at

305　ambient temperature. The dynamic calculations show specifically that the stability of form II

306　arises as a result of its greater vibrational entropy. However, two caveats apply: (1) the free

307　energy calculation is based on the harmonic approximation, which would be expected to

308　influence the predicted value of the transition point; (2) the calculations refer to the idealised

16

309    form I and form II crystal structures, and do not consider structural disorder associated with the

310    intergrown nature of form I / form II single crystals.

## 311    4    Conclusions

312    This work applies THz-TDS and ab initio simulations to explore the two highly similar

313    polymorphs of aspirin. The results show that, even for these two nearly identical crystal

314    structures, THz-TDS can reveal spectral differences based on its sensitivity to inter- and intra-

315    molecular forces. With the help of DFT simulations, slight differences observed for the aspirin

316    polymorphs and the spectra provide further solid evidence of the intergrown nature of the two

317    forms. A number of calculated physical properties are compared for the two forms and most of

318    them are found to be quite similar, reflecting the high degree of structural similarity. However,

319    form II shows a relatively larger vibrational entropy, which yields a lower free energy than form

320    I at temperatures above 75 K. Larger parameters for the baseline fitting of the THz-TDS spectra

321    also indicate a higher degree of structural disorder for form II, consistent with established

322    expectations for this polymorph. Further computational work on a supercell structure

323    incorporating defects would be very valuable to investigate the influence of structural

324    imperfections in the system and could also add insight into possible phase transitions between

325    the aspirin polymorphs. However, a highly efficient computational plan will be required as well

326    as a large amount of computational resource to pursue this work further.

**References**

(1) Wheatley, P. J. 1163. The Crystal and Molecular Structure of Aspirin. *Journal of the Chemical Society (Resumed)* **1964**, 6036. https://doi.org/10.1039/jr9640006036.

(2) Vishweshwar, P.; McMahon, J. A.; Oliveira, M.; Peterson, M. L.; Zaworotko, M. J. The Predictably Elusive Form II of Aspirin. *Journal of the American Chemical Society* **2005**, *127* (48), 16802–16803. https://doi.org/10.1021/ja056455b.

(3) Ouvrard, C.; Price, S. L. Toward Crystal Structure Prediction for Conformationally Flexible Molecules: The Headaches Illustrated by Aspirin. *Crystal Growth & Design* **2004**, *4* (6), 1119–1127. https://doi.org/10.1021/cg049922u.

(4) Bond, A. D.; Boese, R.; Desiraju, G. R. On the Polymorphism of Aspirin. *Angewandte Chemie International Edition* **2007**, *46* (4), 615–617. https://doi.org/10.1002/anie.200602378.

(5) Bond, A. D.; Boese, R.; Desiraju, G. R. On the Polymorphism of Aspirin: Crystalline Aspirin as Intergrowths of Two "Polymorphic" Domains. *Angewandte Chemie International Edition* **2007**, *46* (4), 618–622. https://doi.org/10.1002/anie.200603373.

(6) Bond, A. D.; Solanko, K. A.; Parsons, S.; Redder, S.; Boese, R. Single Crystals of Aspirin Form II: Crystallisation and Stability. *CrystEngComm* **2011**, *13* (2), 399–401. https://doi.org/10.1039/C0CE00588F.

(7) Shtukenberg, A. G.; Hu, C. T.; Zhu, Q.; Schmidt, M. U.; Xu, W.; Tan, M.; Kahr, B. The Third Ambient Aspirin Polymorph. *Crystal Growth & Design* **2017**, *17* (6), 3562–3566. https://doi.org/10.1021/acs.cgd.7b00673.

(8) Polytypism - Online Dictionary of Crystallography https://dictionary.iucr.org/Polytypism (accessed Aug 7, 2021).

(9)     Wen, S.; Beran, G. J. O. Accidental Degeneracy in Crystalline Aspirin: New Insights from High-Level Ab Initio Calculations. *Crystal Growth & Design* **2012**, *12* (5), 2169–2172. https://doi.org/10.1021/cg300358n.

(10)    Reilly, A. M.; Tkatchenko, A. Role of Dispersion Interactions in the Polymorphism and Entropic Stabilization of the Aspirin Crystal. *Physical Review Letters* **2014**, *113* (5), 055701. https://doi.org/10.1103/PhysRevLett.113.055701.

(11)    Vaksler, Y.; Idrissi, A.; Urzhuntseva, V. v.; Shishkina, S. v. Quantum Chemical Modeling of Mechanical Properties of Aspirin Polymorphic Modifications. *Crystal Growth and Design* **2021**, *21* (4). https://doi.org/10.1021/acs.cgd.0c01613.

(12)    Turner, M. J.; Thomas, S. P.; Shi, M. W.; Jayatilaka, D.; Spackman, M. A. Energy Frameworks: Insights into Interaction Anisotropy and the Mechanical Properties of Molecular Crystals. *Chemical Communications* **2015**, *51* (18), 3735–3738. https://doi.org/10.1039/C4CC09074H.

(13)    Chan, E. J.; Welberry, T. R.; Heerdegen, A. P.; Goossens, D. J. Diffuse Scattering Study of Aspirin Forms (I) and (II). *Acta Crystallographica Section B: Structural Science* **2010**, *66* (6), 696–707. https://doi.org/10.1107/S0108768110037055/SO5043SUP1.CIF.

(14)    King, M. D.; Buchanan, W. D.; Korter, T. M. Identification and Quantification of Polymorphism in the Pharmaceutical Compound Diclofenac Acid by Terahertz Spectroscopy and Solid-State Density Functional Theory. *Analytical Chemistry* **2011**, *83* (10), 3786–3792. https://doi.org/10.1021/ac2001934.

(15)    King, M. D.; Buchanan, W. D.; Korter, T. M. Understanding the Terahertz Spectra of Crystalline Pharmaceuticals: Terahertz Spectroscopy and Solid-State Density Functional Theory Study of (S)-(+)-Ibuprofen and (RS)-Ibuprofen. *Journal of Pharmaceutical Sciences* **2011**, *100* (3), 1116–1129. https://doi.org/10.1002/jps.22339.

(16) Zeitler, J. A.; Newnham, D. A.; Taday, P. F.; Threlfall, T. L.; Lancaster, R. W.; Berg, R. W.; Strachan, C. J.; Pepper, M.; Gordon, K. C.; Rades, T. Characterization of Temperature-Induced Phase Transitions in Five Polymorphic Forms of Sulfathiazole by Terahertz Pulsed Spectroscopy and Differential Scanning Calorimetry. *Journal of Pharmaceutical Sciences* **2006**, *95* (11), 2486–2498. https://doi.org/10.1002/jps.20719.

(17) Ruggiero, M. T.; Sibik, J.; Zeitler, J. A.; Korter, T. M. Examination of <scp>l</Scp> -Glutamic Acid Polymorphs by Solid-State Density Functional Theory and Terahertz Spectroscopy. *The Journal of Physical Chemistry A* **2016**, *120* (38), 7490–7495. https://doi.org/10.1021/acs.jpca.6b05702.

(18) Laman, N.; Harsha, S. S.; Grischkowsky, D. Narrow-Line Waveguide Terahertz Time-Domain Spectroscopy of Aspirin and Aspirin Precursors. *Applied Spectroscopy* **2008**, *62* (3), 319–326. https://doi.org/10.1366/000370208783759768.

(19) Dovesi, R.; Erba, A.; Orlando, R.; Zicovich-Wilson, C. M.; Civalleri, B.; Maschio, L.; Rérat, M.; Casassa, S.; Baima, J.; Salustro, S.; Kirtman, B. Quantum-mechanical Condensed Matter Simulations with CRYSTAL. *WIREs Computational Molecular Science* **2018**, *8* (4), e1360. https://doi.org/10.1002/wcms.1360.

(20) Groom, C. R.; Bruno, I. J.; Lightfoot, M. P.; Ward, S. C. The Cambridge Structural Database. *Acta Crystallographica Section B Structural Science, Crystal Engineering and Materials* **2016**, *72* (2), 171–179. https://doi.org/10.1107/S2052520616003954.

(21) Wilson, C. C. Interesting Proton Behaviour in Molecular Structures. Variable Temperature Neutron Diffraction and Ab Initio Study of Acetylsalicylic Acid: Characterising Librational Motions and Comparing Protons in Different Hydrogen Bonding PotentialsElectronic Supplementary Information (ESI) Available: Bond Lengths and Angles from the Refinements, Refined Atomic Coordinates and ADPs. See

Http://Www.Rsc.Org/Suppdata/Nj/B2/B203775k/. *New Journal of Chemistry* **2002**, *26* (12), 1733–1739. https://doi.org/10.1039/b203775k.

(22)    Schäfer, A.; Horn, H.; Ahlrichs, R. Fully Optimized Contracted Gaussian Basis Sets for Atoms Li to Kr. *The Journal of Chemical Physics* **1992**, *97* (4), 2571–2577. https://doi.org/10.1063/1.463096.

(23)    Perdew, J. P.; Burke, K.; Ernzerhof, M. Generalized Gradient Approximation Made Simple. *Physical Review Letters* **1996**, *77* (18), 3865–3868. https://doi.org/10.1103/PhysRevLett.77.3865.

(24)    Grimme, S.; Antony, J.; Ehrlich, S.; Krieg, H. A Consistent and Accurate *Ab Initio* Parametrization of Density Functional Dispersion Correction (DFT-D) for the 94 Elements H-Pu. *The Journal of Chemical Physics* **2010**, *132* (15), 154104. https://doi.org/10.1063/1.3382344.

(25)    Grimme, S.; Ehrlich, S.; Goerigk, L. Effect of the Damping Function in Dispersion Corrected Density Functional Theory. *Journal of Computational Chemistry* **2011**, *32* (7), 1456–1465. https://doi.org/10.1002/jcc.21759.

(26)    Donà, L.; Brandenburg, J. G.; Bush, I. J.; Civalleri, B. Cost-Effective Composite Methods for Large-Scale Solid-State Calculations. *Faraday Discussions* **2020**, *224*, 292–308. https://doi.org/10.1039/D0FD00066C.

(27)    Noel, Y.; Zicovich-Wilson, C. M.; Civalleri, B.; D'Arco, Ph.; Dovesi, R. Polarization Properties of ZnO and BeO:  An *Ab Initio* Study through the Berry Phase and Wannier Functions Approaches. *Physical Review B* **2001**, *65* (1), 014111. https://doi.org/10.1103/PhysRevB.65.014111.

(28)    Pascale, F.; Zicovich-Wilson, C. M.; López Gejo, F.; Civalleri, B.; Orlando, R.; Dovesi, R. The Calculation of the Vibrational Frequencies of Crystalline Compounds and Its

Implementation in the CRYSTAL Code. *Journal of Computational Chemistry* **2004**, *25* (6), 888–897. https://doi.org/10.1002/jcc.20019.

(29)     Boys, S. F.; Bernardi, F. The Calculation of Small Molecular Interactions by the Differences of Separate Total Energies. Some Procedures with Reduced Errors. *Molecular Physics* **2002**, *100* (1), 65–73. https://doi.org/10.1080/00268970110088901.

(30)     Jepsen, P. U.; Fischer, B. M. Dynamic Range in Terahertz Time-Domain Transmission and Reflection Spectroscopy. *Optics Letters* **2005**, *30* (1), 29. https://doi.org/10.1364/OL.30.000029.

(31)     Sibik, J.; Zeitler, J. A. Direct Measurement of Molecular Mobility and Crystallisation of Amorphous Pharmaceuticals Using Terahertz Spectroscopy. *Advanced Drug Delivery Reviews*. 2016. https://doi.org/10.1016/j.addr.2015.12.021.

(32)     Tan, N. Y.; Zeitler, J. A. Probing Phase Transitions in Simvastatin with Terahertz Time-Domain Spectroscopy. *Molecular Pharmaceutics* **2015**, *12* (3). https://doi.org/10.1021/mp500649q.

(33)     Nickel, D. v.; Ruggiero, M. T.; Korter, T. M.; Mittleman, D. M. Terahertz Disorder-Localized Rotational Modes and Lattice Vibrational Modes in the Orientationally-Disordered and Ordered Phases of Camphor. *Physical Chemistry Chemical Physics* **2015**, *17* (10). https://doi.org/10.1039/c4cp04947k.

# Graphical TOC Entry



**Form I**

**Form II**